Supporting Information

Predicting two-dimensional semiconducting boron carbides

Xinxin Tian[†], *Xiaoyu Xuan*[‡], *Yu Meng*[§], *Yuewen Mu*[*,†], *Hai-Gang Lu*[†], *Zhuhua Zhang*[*,‡], *Si-Dian Li*[*,†]

† Institute of Molecular Science, Key Laboratory of Materials for Energy Conversion and Storage of Shanxi Province, Shanxi University, Taiyuan 030006, P. R. China

‡ State Key Laboratory of Mechanics and Control of Mechanical Structures, Key Laboratory for Intelligent Nano Materials and Devices of Ministry of Education and Institute of Nano Science, Nanjing University of Aeronautics and Astronautics, Nanjing 210016, China

§ School of chemistry and chemical engineering, Yulin University, Yulin, 719000, P. R. China

To whom correspondence should be addressed Email: ywmu@sxu.edu.cn, chuwazhang@nuaa.edu.cn, lisidian@sxu.edu.cn

Other structural details of B_4C_3 monolayer:

There are three types of B-B bonds: the bonds formed by periphery B atom with the center B atom are 1.565 and 1.575 Å, respectively; the bonds along the hexagonal periphery of each B_4C_3 unit are 1.584, 1.586 and 1.587 Å, respectively; the bonds fusing B_4C_3 unit are 1.529 and 1.534 Å, respectively. The two symmetrically distinct B-C distances are 1.730 and 1.729 Å, respectively.

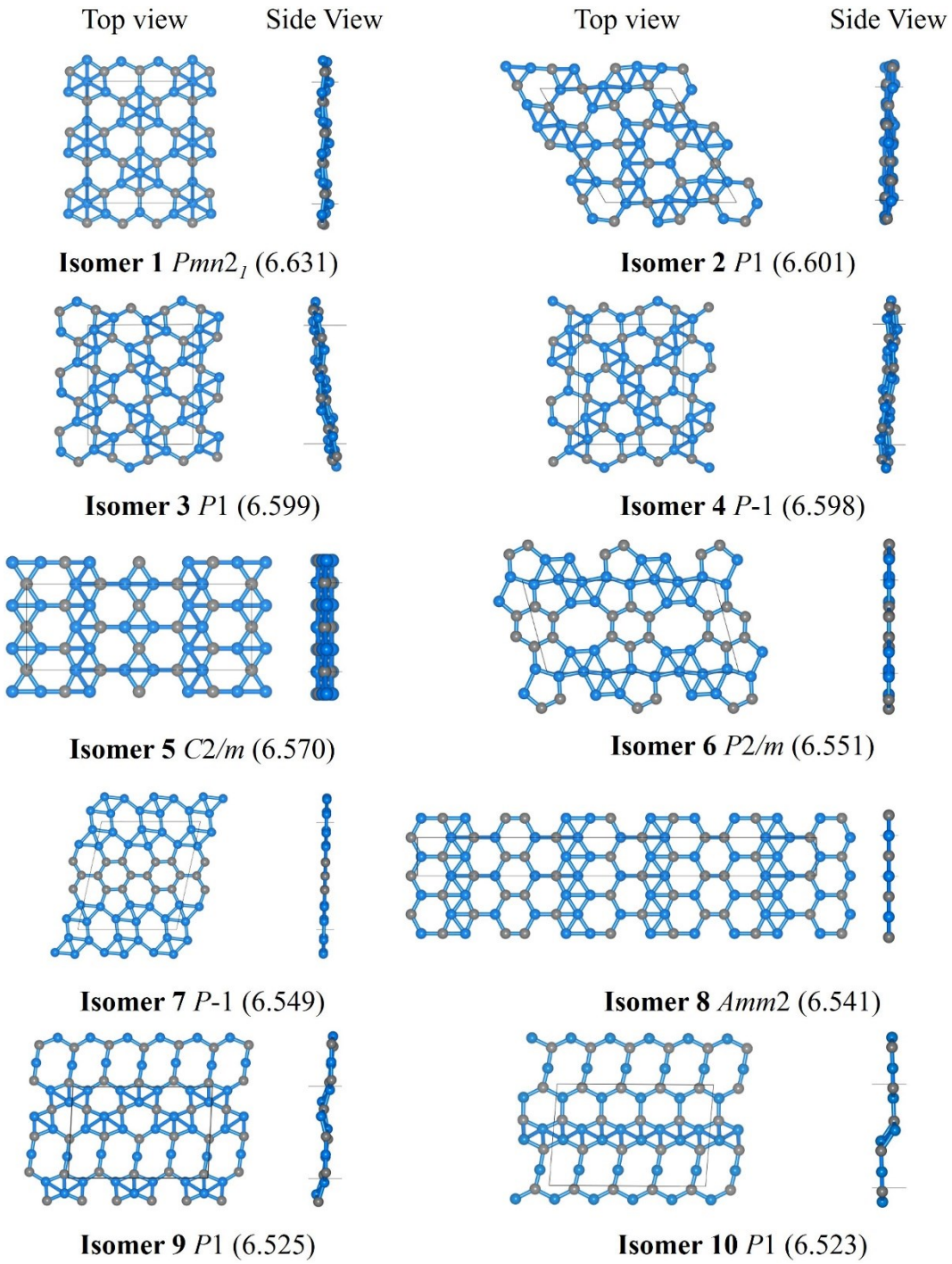

Fig. S1. Optimized atomic geometries, space groups and cohesive energies (eV/atom) of the first 10 low-lying B_4C_3 monolayers.

B_4C_3 unit isolated structures:

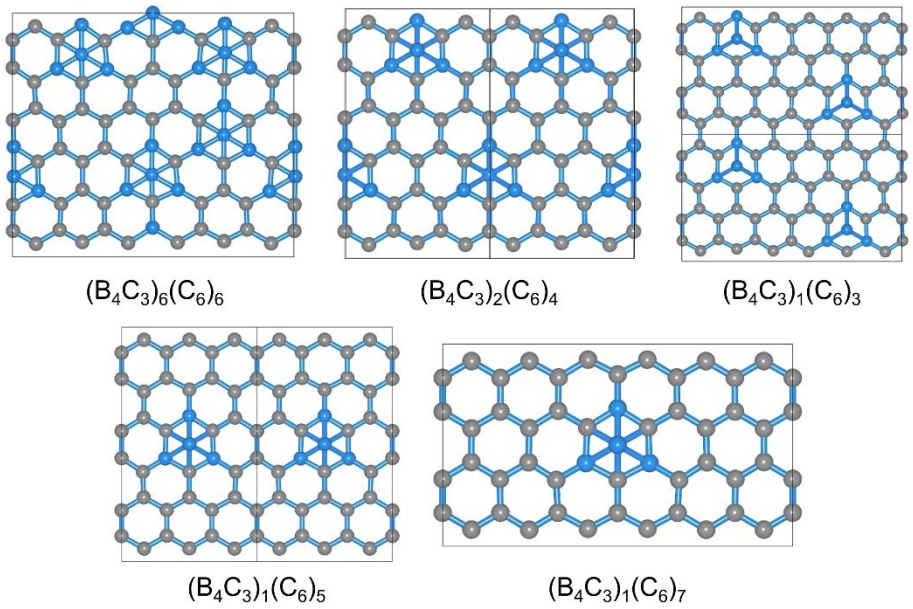

Heterojunction structures:

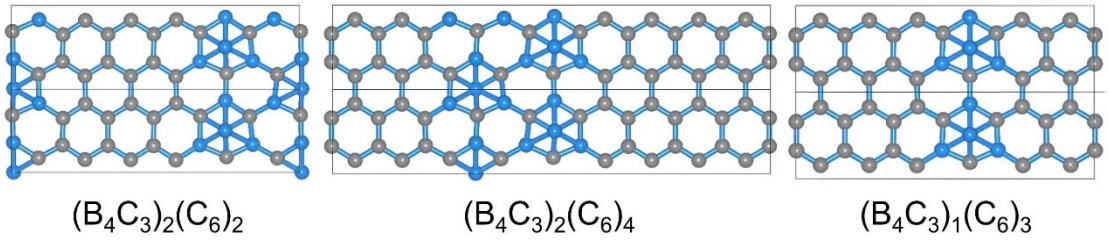

$(B_4C_3)_3(C_6)_6$ BN-type:

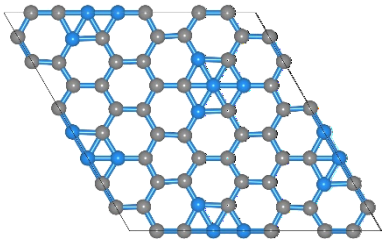

Fig. S2. Optimized atomic geometries of $(B_4C_3)_m(C_6)_n$ (n/m=1-7) monolayers.

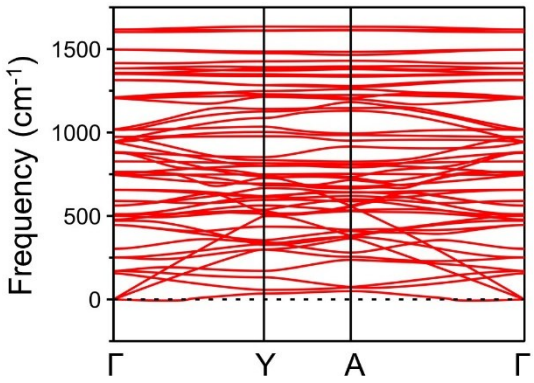

Fig. S3 Phonon spectrum of the $(B_4C_3)_3(C_6)_6$ monolayer. Γ, Y and A correspond to the k-points (0, 0, 0), (0, 0.5, 0) and (-0.3333, 0.6667, 0) in the first Brillouin zone.

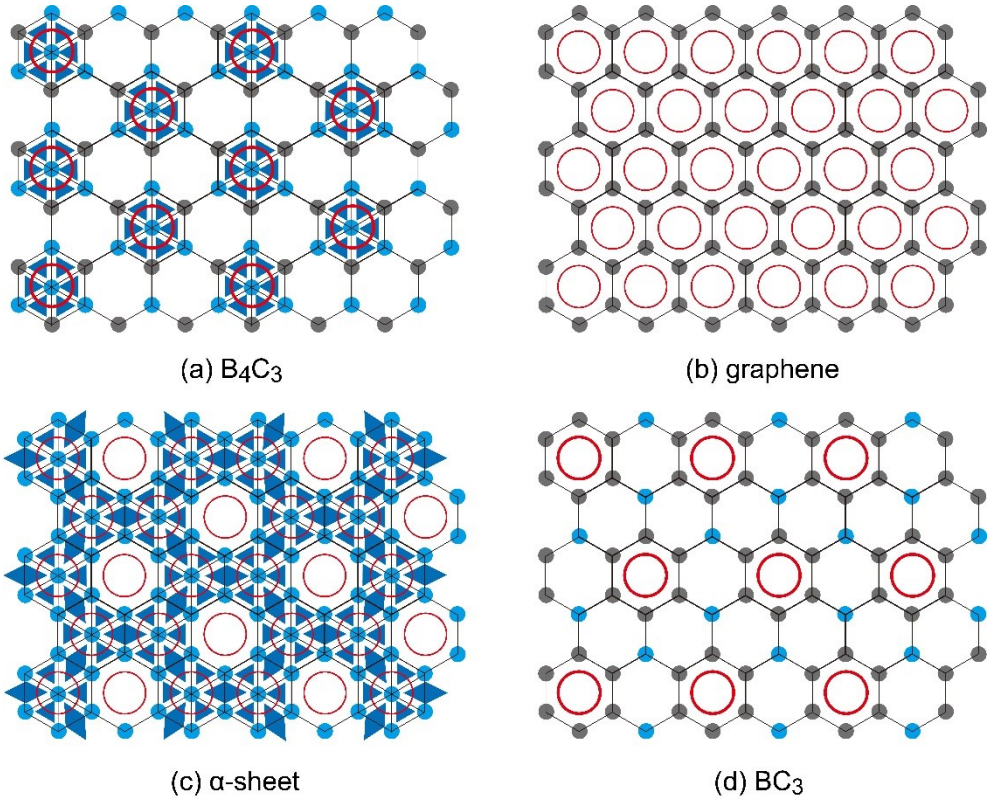

Fig. S4 π bonding patterns of (a) B_4C_3 (b) graphene (c) α-sheet (d) BC_3 monolayers. The thin and thick red circles represent one and three delocalized π bonds, respectively.

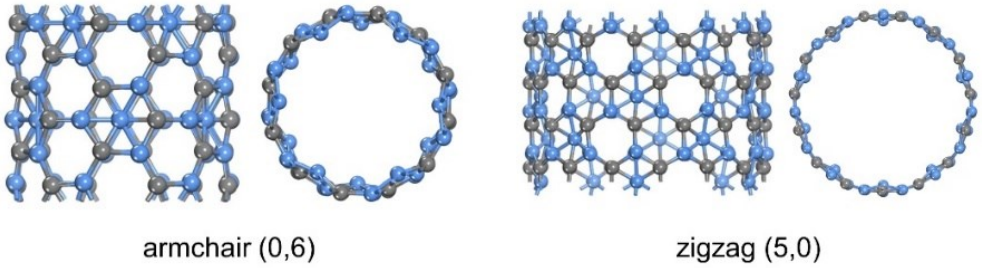

Fig. S5 Structures of nanotubes rolled from B_4C_3 sheet: the armchair (0,6) and zigzag (5,0) are shown as examples.

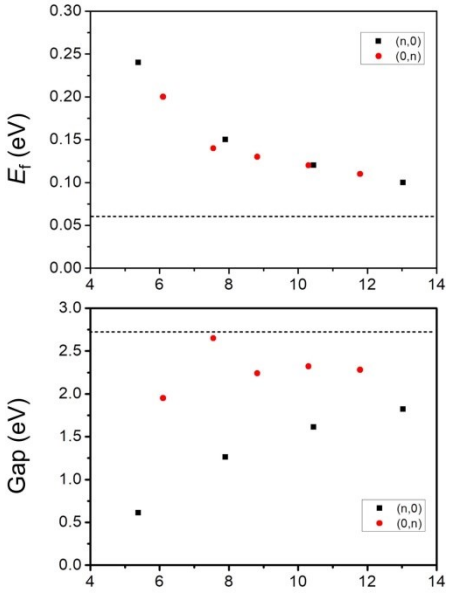

Fig. S6 The formation energies (E_f) and the band gaps of B_4C_3 nanotubes vs the diameters d (Å). The dash line represents the value of proposed B_4C_3 monolayer.

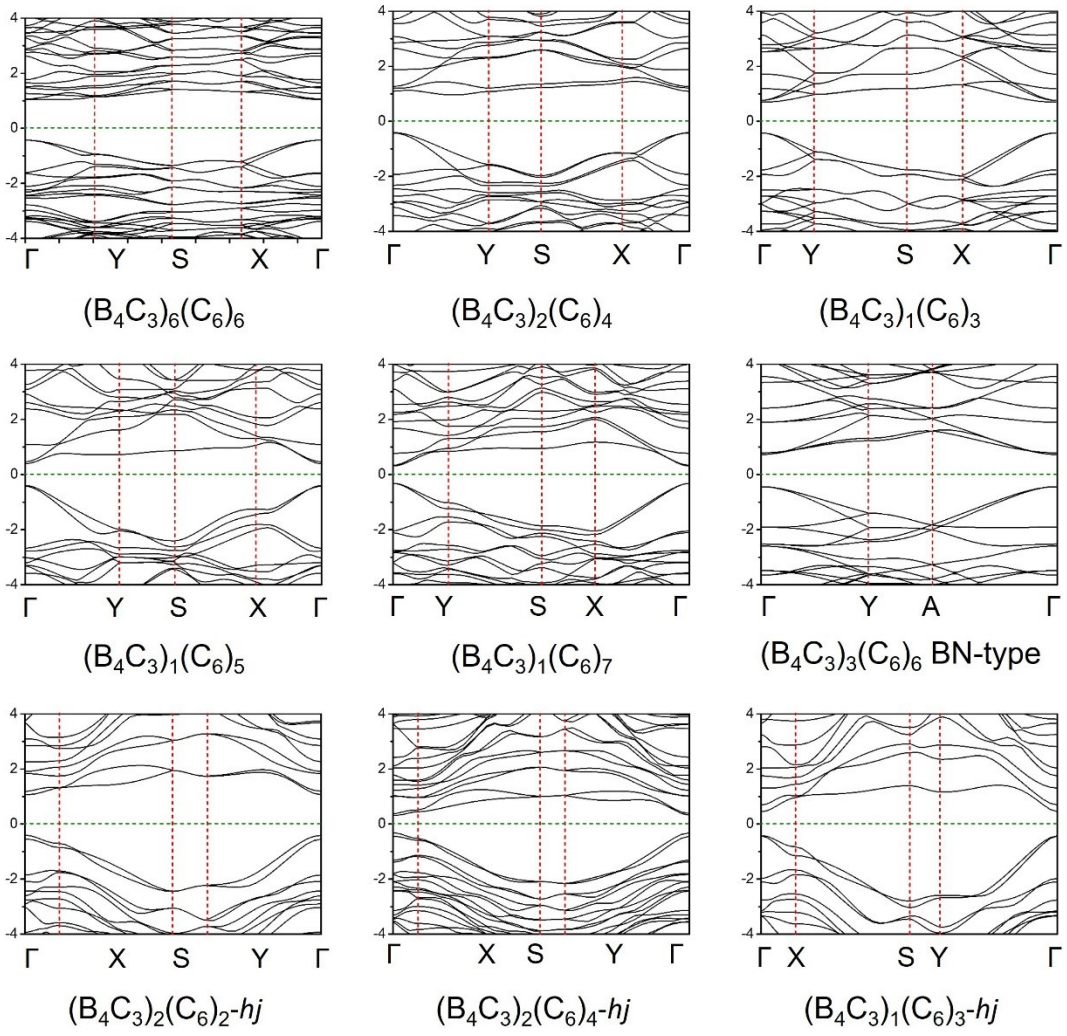

Fig. S7 Band structures of the $(B_4C_3)_m(C_6)_n$ (n/m=1-7) monolayers at HSE06 level. Γ, Y, S, X and A correspond to the k-points (0, 0, 0), (0, 0.5, 0), (0.5, 0.5, 0), (0.5, 0, 0) and (-0.3333, 0.6667, 0) in the first Brillouin zone. *hj* represents heterojunction structure. The band structure of $(B_4C_3)_2(C_6)_4$-*hj* at PBE level was used due to its large number of atoms in the supercell and thus a high computational cost of HSE06 functional.

Table S1. Formation energies (E_f, eV/atom) of B_nC_m monolayers and $(B_4C_3)_m(C_6)_n$ (n/m=1-7) family refer to the average energies per atom of α-boron sheet and graphene.

Composition	E_f	**Composition**	E_f
BC	0.16	BC_2	0.19
B_2C	0.16	BC_3	0.10
B_3C	0.09	BC_5	0.09
B_5C	0.14	B_4C_3	0.06
$(B_4C_3)_6(C_6)_6$	0.19	$(B_4C_3)_2(C_6)_2$ heterojunction	0.12
$(B_4C_3)_2(C_6)_4$	0.16	$(B_4C_3)_2(C_6)_4$ heterojunction	0.10
$(B_4C_3)_1(C_6)_3$	0.11	$(B_4C_3)_1(C_6)_3$ heterojunction	0.09
$(B_4C_3)_1(C_6)_5$	0.11	$(B_4C_3)_3(C_6)_6$ BN-type	0.18
$(B_4C_3)_1(C_6)_7$	0.09		

Table S2. Calculated diameters *d* (Å), average formation energies per atom (eV) (PBE level) and the bandgaps (HSE06 level) of B_4C_3 nanotubes.

B_4C_3 nanotube	***d* (Å)**	**E_f (eV)**	**Gap (eV)**
(2,0)	5.39	0.24	0.61
(3,0)	7.90	0.15	1.26
(4,0)	10.45	0.12	1.61
(5,0)	13.03	0.10	1.82
(0,4)	6.10	0.20	1.95
(0,5)	7.55	0.14	2.65
(0,6)	8.82	0.13	2.24
(0,7)	10.30	0.12	2.32
(0,8)	11.79	0.11	2.28